hydrology

MDPI

Article

Modeling the Impacts of Sea Level Rise Scenarios on the Amazon River Estuary

Jonathan Luz P. Crizanto [1], Carlos Henrique M. de Abreu [2,3], Everaldo B. de Souza [4] and Alan C. da Cunha [1,3,5,*]

[1] Graduate Program in Tropical Biodiversity (PPGBIO), Federal University of Amapá (UNIFAP), Macapá 68902-280, AP, Brazil; jonathanluz3@gmail.com
[2] Environmental Engineering School (CEAM), Amapá State University (UEAP), Macapá 68900-070, AP, Brazil; carlos.abreu@ueap.edu.br
[3] Graduate Program in Biotechnology (Bionorte), Federal University of Amapá (UNIFAP), Macapá 68902-280, AP, Brazil
[4] Institute of Geosciences, Federal University of Pará (UFPA), Belém 66075-111, PA, Brazil; everaldo@ufpa.br
[5] Civil Engineering Department, Federal University of Amapá (UNIFAP), Macapá 68902-280, AP, Brazil
* Correspondence: alancunha@unifap.br

Abstract: The rise in the global mean sea level (MSL) is a significant consequence of climate change, attributed to both natural and anthropogenic forces. This phenomenon directly affects the dynamic equilibrium of Earth's oceanic and estuarine ecosystems, particularly impacting the Amazon estuary. In this study, a numerical model was employed to investigate the long-term impacts of MSL fluctuations on key hydrodynamic parameters crucial to regional environmental dynamics. Our investigation was based on scenarios derived from Representative Concentration Pathways (RCPs) and Coupled Model Intercomparison Project Phase 5 (CMIP5) projections, incorporating MSL variations ranging from 30 to 150 cm above the current mean level. Following careful calibration and validation procedures, which utilized observational and in situ data, notably from field expeditions conducted in 2019, our simulations unveiled significant impacts on certain hydrodynamic parameters. Specifically, we observed a pronounced increase in diurnal tidal amplitude ($p < 0.05$) within the upstream sections of the North and South channels. Additionally, discernible alterations in water renewal rates throughout the estuary were noted, persisting for approximately 2 days during the dry season ($p < 0.05$). These findings provide valuable insights into the vulnerability of key parameters to hydrologic instability within the Amazonian coastal region. In conclusion, this study represents a pivotal scientific endeavor aimed at enhancing the preservation of aquatic ecosystems and advancing the environmental knowledge of the Lower Amazon River, with the goal of proactively informing measures to safeguard the current and future sustainability of these vital ecosystems.

Keywords: Amazon estuary; tide; transport time; climate change; numerical model

Citation: Crizanto, J.L.P.; de Abreu, C.H.M.; de Souza, E.B.; da Cunha, A.C. Modeling the Impacts of Sea Level Rise Scenarios on the Amazon River Estuary. *Hydrology* **2024**, *11*, 86. https://doi.org/10.3390/hydrology11060086

Academic Editor: Serter Atabay

Received: 12 April 2024
Revised: 21 May 2024
Accepted: 31 May 2024
Published: 20 June 2024

1. Introduction

The global mean sea level, driven by climate change, increased from 11 to 16 cm in the 20th century [1] and, even with an abrupt and immediate cut in greenhouse gas emissions, it could increase by another 50 cm by the end of the 21st century [2]. In higher emission scenarios, the rise over the century may approach extreme levels and exceed 200 cm if some early instability of the Antarctic ice sheet occurs [3]. During the last century, the global sea level rise was driven by melting glaciers, rising groundwaters and thermal expansion of the oceans [4]. This rise in mean sea level (SLR) not only generates responses such as increased coastal salinity [5,6] and ocean currents [7], but also causes changes in physical parameters in coastal systems such as residence times and transport of passive substances in the runoff [8]. Such effects can change according to the different types of estuaries, which are related to their physical characteristics, especially bathymetry, length, and geometry [9].

Therefore, each coastal region has unique physical characteristics, whose response to the sea level rise depends on local geological, morphological, and atmospheric conditions.

Indeed, hydrodynamic conditions are elementary and fundamental to evaluate the equilibrium or vulnerability conditions of aquatic ecosystems and their relationship with the conservation and management of biodiversity, especially in the context of climate change. For example, most measurements of microbial respiration in large rivers ignore the influence of runoff on the reaction rates, tending to underestimate the contribution of these processes to the CO_2 emitted into the atmosphere, as occurs in the Amazon River. These aspects have already been shown in experimental studies reporting that the flow velocity and hydrodynamic conditions are key factors that control the microbial metabolism of metabolized organic matter in the aquatic system itself [10]. Therefore, microbial respiration can potentially exceed the CO_2 emission rates in the main channels and be balanced by primary production, atmospheric emissions and other inputs into mass balances [11].

The Amazon basin drains an area of approximately 6.5 million km^2, representing ~16–20% of the global freshwater discharge to the ocean and ~44% of the global flow of CO_2 gas emitted from inland waters [12–14]. In addition, its plume extends up to 106 km^2 over the Western Tropical North Atlantic (WTNA), being carried northwest by the North Brazil Current (NBC) along the coast of the northern Brazilian shelf [15]. In this context, the Amazon River estuary presents unique hydrodynamic conditions, distinct from those of other estuaries on the planet, that have proved to be extremely challenging and complex in terms of logistics, field experimental approach and even the use and application of numerical models, including hydrodynamics, water quality and matter flows [16,17]. This complexity arises primarily from the increasing recognition of inland waters and coastal oceans as integrated systems, constantly transporting and transforming biogeochemical constituents [18]. The result of this interaction has been the generation of unique aquatic habitats that, in turn, dynamically shape and influence different ecosystems along the continuum [19,20]. However, few studies have approached questions about the potential impacts of the SLR on the hydrodynamic spatiotemporal patterns in the natural flow of the Amazon River Estuary. The estuarine hydrology is related to the main control factors of carbon fluxes and emissions and the transport of nutrients and sediments in this delicate and dynamic boundary between the continuum of river systems (Amazonas) and receiving oceanic waters (Atlantic) [21]. For example, rivers generally act as a CO_2 emission pump that transfers carbon dioxide from water to the atmosphere [12] where, usually, part of this transfer happens due to the decomposition of terrestrial organic matter [18] and inputs from the floodplains [21,22]. On the other hand, in coastal areas dominated by rivers, such as the plume of the Amazon River (ARP), the simultaneous removal of CO_2 from the atmosphere can also occur due to the increase in primary production driven by the presence of river nutrients [15]. Thus, hydrodynamics in this zone tends to control the mass and energy fluxes, also influencing the behavior of the saline interface itself, defining the river–ocean limits [10], because the hydrodynamic approach is complex due to its gigantic scale and experimental limitations. However, these experimental limitations justify the scarcity of broad studies in this region. Nonetheless, they present a significant opportunity to leverage numerical modeling and simulation techniques in conjunction with experimental data [15,23,24]. This approach allows for the representation of the entire system, encompassing not only boundary conditions and local hydrology but also the influence of oceanic tides and circulation hydrodynamics. Furthermore, it facilitates the study of spatio-temporal variations, such as tidal amplitudes, currents and discharges, utilizing current observational data and/or future climate projections as criteria. Therefore, it is possible to test hypotheses related to water balances and their potential influences on the concentrations of constituents such as nutrients or passive substances within these hyperdynamic zones [25].

Here, we employ an efficient and suitable numerical model to investigate the potential regional extreme impacts of long-term sea level rise (SLR) scenarios on the coastal hydrodynamic patterns of the Lower Amazon River. The focus is on examining the spatiotemporal

patterns of tide and surface water renewal rates during both wet and dry regimes. The SISBAHIA model [26], which has been commonly utilized in similar applications within the Amazon River estuary [16,17,27], is employed for this study. Considering the projections until the end of the century from different CMIP5 RCPs scenarios, we hypothesize a SLR ranging from 30 to 150 cm above the current mean level in the Amazonian estuary. As a general hypothesis, based on previous hydrodynamic knowledge of the Amazon River estuary, we expect that the moderate geometric convergence of the channel will result in a gradual increase in the tidal range as it propagates upstream. This hypothesis has been investigated in other regions of the globe, such as in the studies by [7], who investigated the rise in sea level and its influence on freshwater flows and on the estuarine circulation pattern in EUA.

Therefore, our research stands out for its focused exploration of the hydrodynamics of the Amazon estuary, a topic rarely addressed in previous studies. This uniqueness encompasses both our methodological approach, which utilizes advanced hydrodynamic and environmental numerical modeling techniques, and the integration of IPCC scenarios to assess the current and projected impacts of sea level rise on these coastal regions. Additionally, our investigation provides unprecedented insights into the potential effects of sea level rise disturbances on hydrodynamic parameters, meticulously documenting these variations. Through this endeavor, we aim to raise awareness among the scientific community and resource managers about the ecological implications for estuarine ecosystems within the Amazon River plume.

2. Materials and Methods

2.1. Study Area

The study area (Figure 1) covered the eastern Amazon, from the city of Óbidos in the state of Pará to the mouth of the Amazon basin in the state of Amapá, including the entire coastal zone of the island of Marajó and the adjacent oceanic area over the equatorial Atlantic. This region is characterized by high geographical and hydrological complexity, with the presence of the north and south channel of the Amazon River between the states of Amapá and Pará (Marajó Island). The tidal range in this region induces a water level variation of approximately 3 m in amplitude at the SP station (classified as mesotide). However, as it approaches the mouth, this amplitude increases, reaching up to 4–6 m or more during semidiurnal periods (macro tidal). When the water level in the Atlantic Ocean rises due to daily tidal effects, there is a complete reversal of the water flow, with the influence of level variation up to Óbidos [28]. Even with the tide reversal, due to the gigantic volume of the Amazon River outflow, there are no records of any saline intrusion, at least as far as Macapá. That is, the upstream waters are exclusively fluvial [29]. The climate is hot and humid with pronounced variations in tropical convective activity and precipitation, which are the most important climatic variables in the region [30].

The SISBAHIA describes the inclusion of climatic variables for its simulations comprehensively and accurately. It incorporates relevant meteorological data such as air temperature, relative humidity, solar radiation, wind speed and precipitation, among others, to model the water balance in general. For instance, these climatic variables are input into the SISBAHIA through specific input files containing the time series of observed or estimated meteorological data for the region of interest. Users can provide these data directly to the software or access them through external sources such as local weather stations or climate databases [16,17,24,27,28].

Based on the input climatic information, the SISBAHIA uses algorithms and hydrological models to simulate various processes related to water resource balance, such as evapotranspiration, soil water infiltration, surface runoff and water percolation, to underground aquifers [27]. These simulations provide valuable insights for water management in the estuarine coast, assisting oceanic researchers in decision-making related to water resource and environmental management [16,17,24,26,27].

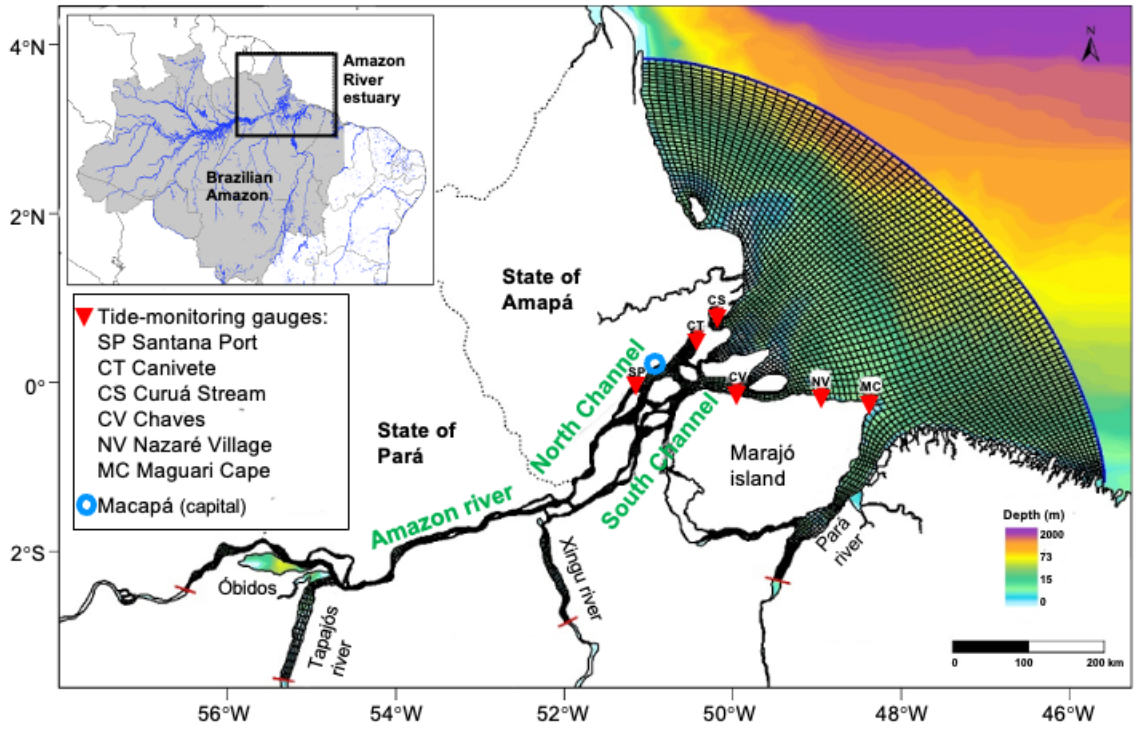

Figure 1. Study area and numerical mesh overlaid on the bathymetric map (shaded) of the Amazon River estuary. The red triangles indicate the tide-monitoring gauges along the coastal region.

In Köppen's classification, the climate is the Am type [31], i.e., tropical rainy monsoon, with a short period presenting rainfall below 80 mm per month (July to December) and average temperature monthly air flow rate of 26.0 ± 0.4 °C, with maximums and minimums between 31.5 ± 0.7 °C and 22.0 ± 0.3 °C, respectively [32,33].

2.2. Definition of Sea Level Rise (SLR) Scenarios

We took into account the future projections of SLR according to the CMIP5 models under different representative concentration pathway (RCP) scenarios [34,35], so that for the period 2081–2100, relative to the current conditions, the expected global mean sea level rise is 0.26 to 0.55 m for RCP2.6, 0.32 to 0.63 m for RCP4.5, 0.33 to 0.63 m for RCP6.0 and 0.45 to 0.82 m for RCP8.5 [2]. Thus, for the present research, we defined the resulting values of SLR by 30 (SLR30), 60 (SLR60), 100 (SLR100) and 150 (SLR150) centimeters above the current mean level in the Amazon River estuary, which is 250 cm according to Brazilian navy data. These four SLR scenarios representative of the end of the 21st century were introduced as input data and boundary conditions of the hydrodynamic model to evaluate the potential impacts on the spatiotemporal patterns of tide, discharge, and water renewal rate in the Amazon estuary region.

2.3. Numerical Model

2.3.1. Hydrodynamic Model

The SISBAHIA (Environmental Hydrodynamics Base System) model, called FIST3D (filtered in space and time 3D), is an efficient three-dimensional hydrodynamic numerical model for large-scale homogeneous flows, composed of two modules. The first module (2DH) calculates vertically averaged currents and free surface elevation. The second module (3D) calculates the three-dimensional velocity field, with two methodology options defined by the user [26]. In addition, in this model, it is possible to include effects of density gradients coupling salt and heat transport models from Water Quality Models and the morphological evolution of the bottom by coupling Sediment Transport, Wave Generation and Propagation Models.

Due to the characteristics of this research, the 2DH hydrodynamic circulation model was chosen, where the basic Equations (1)–(3) consider the flow as "shallow" water, i.e., incompressible, that is, the density within a control volume of moving fluid is considered constant. This same model has already been used efficiently for studies of seed dispersal in rivers (hydrochory) and oil dispersion in the aquatic environment of the Amazon estuarine complex, that is, with flow dynamics, conditions of contour and similar initials [23].

The movement mechanics for turbulent flow in the FIST3D model is governed by the Navier–Stokes equations that represent the principle of momentum conservation and, together with the continuity equation, a state equation and a transport equation for each constituent of the equation of state that makes up the fundamental mathematical model for any body of water:

$$\frac{\partial \zeta}{\partial t} + \frac{\partial UH}{\partial x} + \frac{\partial VH}{\partial y} = q_p + q_E \pm q_I \quad (1)$$

where ζ is the elevation of the water surface; U is the velocity on the *x*-axis; V is the velocity on the *y*-axis; H is the instantaneous depth (m); q_p represents effects due to precipitation; q_E represents effects due to evaporation; and q_I represents effects due to infiltration.

The amount of movement along the x and y axis is calculated by:

$$\frac{\partial U}{\partial t} + U\frac{\partial U}{\partial x} + V\frac{\partial U}{\partial y} = -g\frac{\partial \zeta}{\partial x} - \frac{gH}{2\rho_o}\frac{\partial \rho}{\partial x} + \frac{1}{\rho_o H}\left(\frac{\partial (H\overline{\tau}_{xx})}{\partial x} + \frac{\partial (H\overline{\tau}_{xy})}{\partial y}\right) + \frac{1}{\rho_o H}\left(\tau_x^S - \tau_x^B\right) + 2\phi \sin\theta_V - \frac{V}{H}\sum q \quad (2)$$

$$\frac{\partial V}{\partial t} + U\frac{\partial V}{\partial x} + V\frac{\partial V}{\partial y} = -g\frac{\partial \zeta}{\partial y} - \frac{gH}{2\rho_o}\frac{\partial \rho}{\partial y} + \frac{1}{\rho_o H}\left(\frac{\partial (H\overline{\tau}_{xy})}{\partial x} + \frac{\partial (H\overline{\tau}_{yy})}{\partial y}\right) + \frac{1}{\rho_o H}\left(\tau_y^S - \tau_y^B\right) + 2\phi \sin\theta_U - \frac{V}{H}\sum q \quad (3)$$

where ρ_o is the vertically mean water density (kg m^{-3}); ρ is the constant reference density (kg m^{-3}); g is the acceleration due to gravity (m s^{-2}); $\overline{\tau}_{ij}$ is the turbulent tension tensor (kg m^{-1} s^{-2}), with i j representing two dimensions or areas; τ_i^S is the free surface shear tension (kgm^{-1} s^{-2}); ϕ is the angular speed of the Earth (m m^{-1}); θ is the angle of latitude (m m^{-1}); and Σq are terms on the right side of Equation (1), i.e., the sum of effects due to precipitation, evaporation and infiltration (m^3 s^{-1} m^{-2}).

For the numerical processing, a spatially discretized mesh was used, using the finite element method. The geospatial mesh (Figure 1) is responsible for creating the calculation matrix used by the models. For the 2DH model, the vertical discretization of the water column uses finite differences, so that the complete discretization of the domain results in an overlap of finite element meshes, one for each depth level [26]. For this work, a discretized mesh was used for the selected domain with an average spacing of 3 km, within which 1419 elements and 6460 nodes were generated (Figure 1).

2.3.2. Eulerian Model for Transport Simulation

The numerical scheme used to simulate the transport time was the Eulerian type available on the SISBAHIA platform [26], represented by an advective–diffusive transport model:

$$\frac{\partial \widehat{C}}{\partial t} + \widehat{u}_i\frac{\partial \widehat{C}}{\partial x_i} = \frac{1}{H}\frac{\partial}{\partial x_i}\left(H\widehat{D}_{\ddot{y}}^T\frac{\partial \zeta}{\partial x_j}\right) + \sum R_{P\&C} + \frac{1}{H}\left(q_p\left(C_p - \widehat{C}\right) - q_e\left(C_e - \widehat{C}\right)\right) + \frac{1}{H}\left(q_{in}\left(C_{in} - \widehat{C}\right) - q_{ex}\left(C_{ex} - \widehat{C}\right)\right) \quad (4)$$

where $\widehat{C}$ is the mean concentration of the constituent in the water column; $\widehat{u}_i$ is the component of the velocity vector in the vertically mean direction; H is the height of the water column; $\widehat{D}_{\ddot{y}}^T$ is the turbulent diffusion tensor, modeled with an Elder coefficient; $R_{P\&C}$ indicates kinetic reactions of production and consumption; q_p, q_e, q_{in}, q_{ex} are flows per unit area, for precipitation, evaporation, infiltration and exfiltration, respectively.

2.4. Initial Boundary Conditions

2.4.1. Tide Harmonics

For the external boundary conditions of the hydrodynamic model, the main harmonic constants (Table 1) present in the Amazon River estuary were considered [28], which were obtained through the tide analysis and predict module available in SISBAHIA. That is, a harmonic analysis of level registers was performed to obtain the harmonic constants. The tidal levels were obtained from the MC station record, as it is the closest to the oceanic contour of the modeling domain (see Figure 1).

Table 1. Harmonic constants used as boundary condition in the hydrodynamic model.

Components [1]	Amplitude (cm)	Phase (°)	Description
K1	10.4	272	Lunar/solar diurnal
O1	6.3	251	Principal lunar diurnal
P1	3.4	272	Principal solar diurnal
M2	152.7	315	Principal lunar semidiurnal
S2	40.1	354	Principal solar semidiurnal
N2	36.6	292	Larger lunar elliptic semidiurnal
K2	10.9	354	Lunar/solar semidiurnal

[1] Source: BNDO.

Tidal rises and currents are produced by gravitational and centrifugal forces acting on the oceans. These forces are expressed as the tidal potential, which consists of a set of constituents with discrete frequencies, whose amplitudes and phases are well known over time. However, the tide at any point on Earth is affected by bathymetry in the oceans, especially in bays and estuaries, as the forces are modified by local dynamics in the fluid. The frequencies are unchanged, but the amplitudes and phases of each tidal constituent vary locally [36]. The constants M2 and S2 are the most important for the Amazon River estuarine complex, considering that both would be the main responsible factors for a water level variation between 70 and 85%, and represent the syzygy and quadrature cycles [28].

2.4.2. Bathymetry and Roughness

The background roughness values employed in this study were derived from a comprehensive analysis [30]. The authors meticulously surveyed the diverse bathymetric and roughness characteristics of both the North and the South Channels of the Amazon River. Their work also involved a detailed examination of the river's hydrodynamics and its influence on the sediment transport dynamics within the Amazon River. Thus, the background roughness values utilized in this study were sourced from this comprehensive analysis [29].

To define the updated bathymetry of the Amazon River, a systematic digitization of a comprehensive set of nautical charts (Table 2) published by the Brazilian Navy and available at https://www.marinha.mil.br/chm/dados-do-segnav/cartas-raster (accessed on 30 August 2021) was performed. The roughness data were from the studies by [37] and were defined according to the type of sediment at the bottom of the Amazon River estuary (Figure 1).

2.4.3. Initial Water Discharge Conditions

We input the model flow data for the year 2019, provided by the national water agency (available at http://www.snirh.gov.br/hidrotelemetria/serieHistorica.aspx) (accessed on 30 August 2021), from the Óbidos stations (Amazon River), Itaituba (Tapajós River), Altamira (Xingu River) and Tucurui (Pará River). The compiled results of the flow measurements for the year 2019 are summarized in Figure 2, with evidence that a large part of the flow that enters the system is upstream of Óbidos, with its downstream tributaries representing only 10% of the total flow. The flow of the Pará River was inserted because it is connected to the Amazon River by the de Breves strait (Figure 1). It is estimated that 5% of the flow of the Amazon River flows through the Breves strait into the River Pará [38].

Table 2. Seasonal statistical correlation analysis for the tide stations and the model simulations during 2019 wet and dry regimes.

Station	Season	r^2	RMSE (m)	NSE	r	d
Cabo Maguari (MC)	Wet	0.86	0.48	0.75	0.93	0.95
	Dry	0.91	0.43	0.81	0.95	0.96
Curuá Stream (CS)	Wet	0.93	0.32	0.92	0.96	0.98
	Dry	0.92	0.37	0.90	0.96	0.97
Chaves (CV)	Wet	0.89	0.38	0.81	0.94	0.96
	Dry	0.92	0.34	0.85	0.96	0.96
Canivete (CT)	Wet	0.86	0.33	0.84	0.92	0.96
	Dry	0.91	0.31	0.89	0.95	0.97
Nazaré Village (NV)	Wet	0.92	0.35	0.92	0.96	0.98
	Dry	0.92	0.35	0.92	0.96	0.98
Santana Port (SP)	Wet	0.72	0.46	0.73	0.87	0.90
	Dry	0.74	0.44	0.73	0.86	0.90

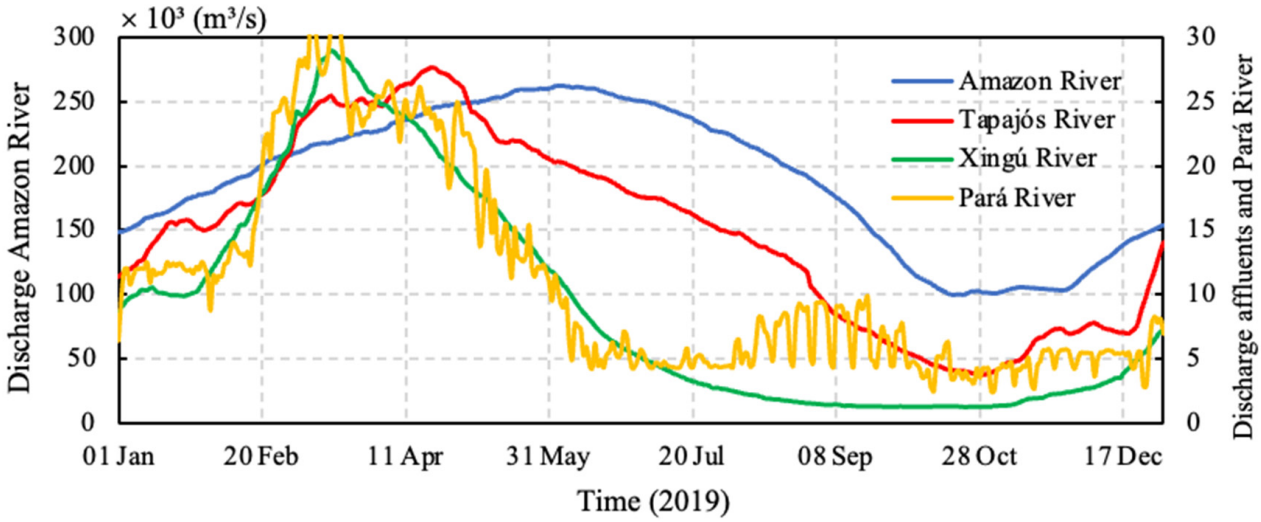

Figure 2. Flow hydrograph for the year 2019 of the Amazon River, its two main tributaries and the Pará River.

2.5. Calibration of the Hydrodynamic Parameters

To evaluate the model's performance and accuracy, the model tidal rise and flow results were compared with experimental and observed data in the field and recorded in the literature by using statistical methods. Due to the scarcity of continuous series of tidal rise data, research on hydrodynamics in the Amazon River estuary poses significant challenges and difficulties for the calibration of models [15,17,23,26,27]. So, even with this limitation, we used tidal elevation data measured by the Brazilian Navy in specific periods at the stations presented in Table 1 and Figure 1. The SISBAHIA tidal forecast module was used to extract the harmonic constants of this tidal rise series, whose objective was to predict the estimated elevation of the water column throughout the year 2019 [26].

2.5.1. Tide Elevation

The comparative statistics results of the observed and simulated tidal rise data are shown in Table 2. The best values of R^2 (0.93) were obtained at the Curuá Stream station (Figure 3). At the remaining stations, this value ranged from 0.72 to 0.92, which is considered acceptable [16,17,23,27]. We also used other tests to confirm the efficiency of the model, such as the Nash Sutcliffe test, the agreement index (d), the Pearson coefficient (r) and the

root-mean-square error (RMSE). Difficulties in the procedures for calibrating tidal variables (try and error procedures) remained a challenge for the Amazon River estuary due to its significant bathymetric heterogeneity [39].

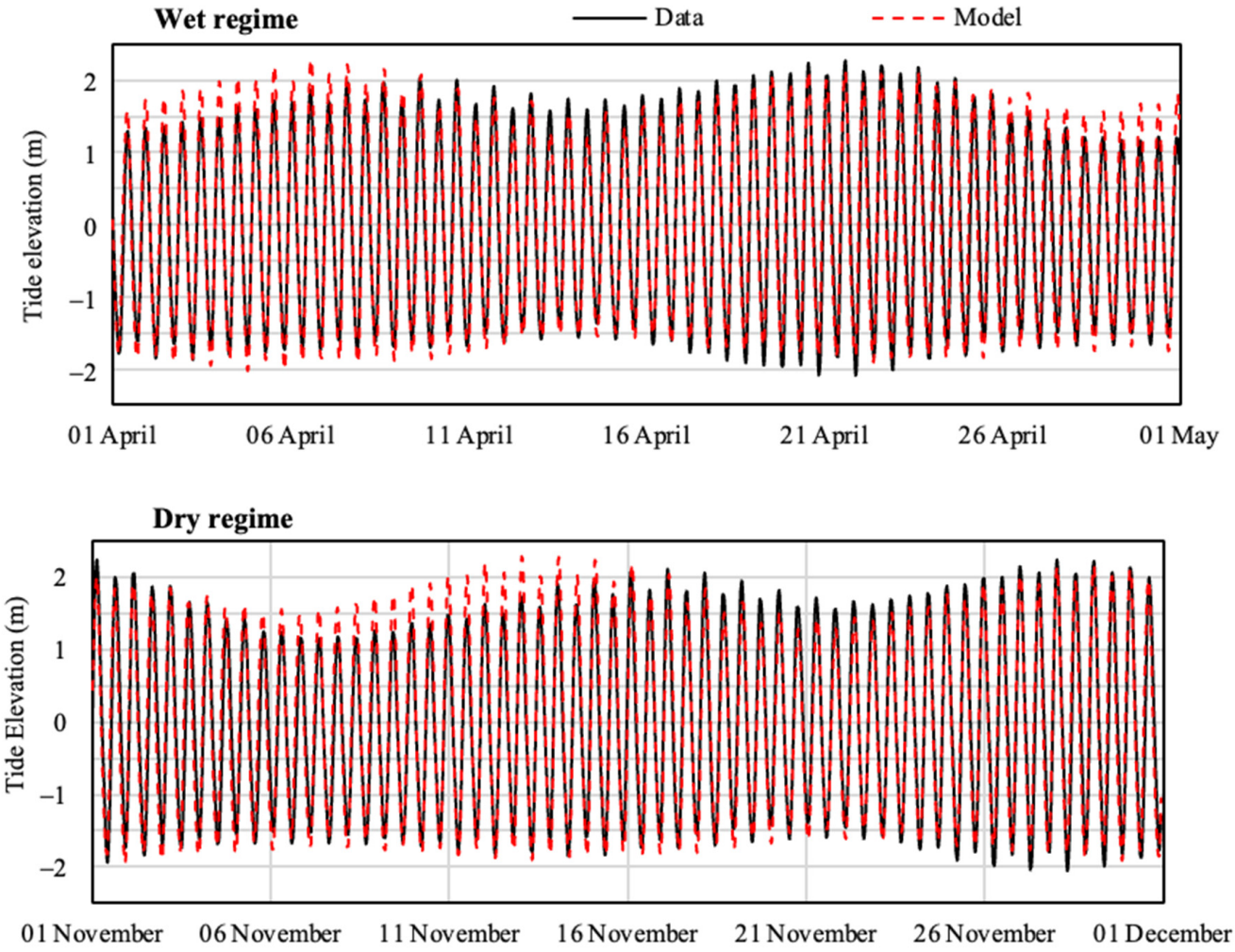

Figure 3. Time series of tide elevation for the CS tide-monitoring gauge in the north channel (black lines) and simulations (red line) during the 2019 wet and dry regimes.

Figure 3 illustrates the observed and simulated tidal time series at the CS tide-monitoring gauge in the north channel, in which it is evident that the model consistently reproduced the temporal hydrodynamics in both seasonal regimes.

2.5.2. Discharge

Figure 4 displays the diurnal variations of river discharge in the north channel in front of Macapá city (location in Figure 1), represented by observational data from a field campaign and model simulations for the 2019 wet (10th April) and dry (12th November) regimes. It is evident that the discharge maximums occurred in the afternoon, and the minimums during the morning in the wet regime, with an inverse pattern in the dry regime, and the temporal behavior was well captured by the model.

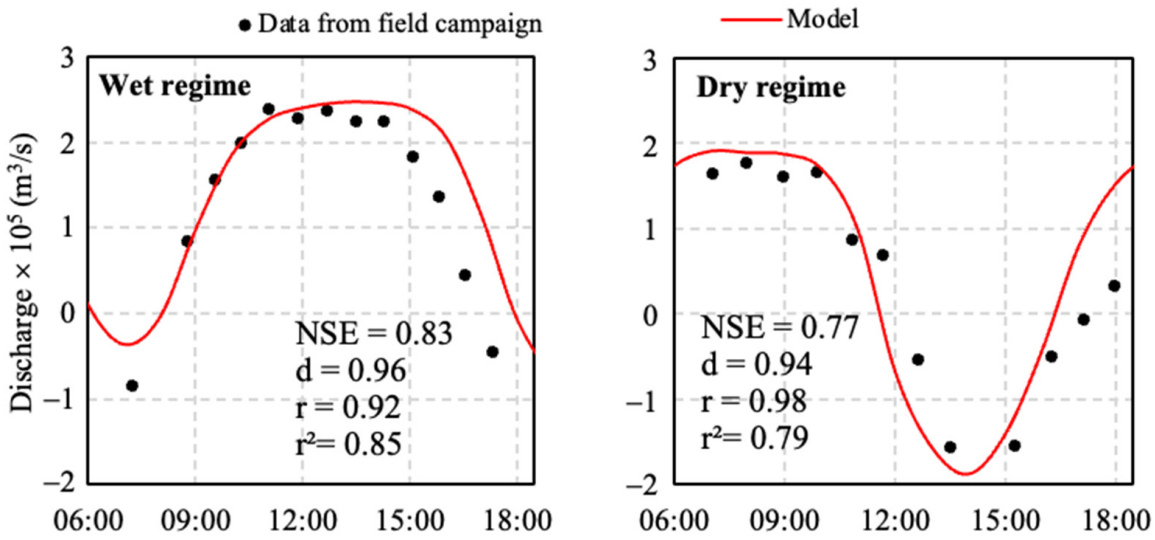

Figure 4. Diurnal variations of river discharge in the north channel in front of Macapá city represented by data from a field campaign and simulations for the 2019 wet (10th April) and dry (12th November) regimes. The statistical test results are highlighted in each period.

3. Results

3.1. Tidal Amplitude Scenarios

Figure 5 shows the diurnal tide amplitude during the wet and dry periods at the CS (north channel) and CV (south channel) tide-monitoring gauges of the Amazon River estuary, considering the current (black line) and the numerical simulations using the SLR (colored lines) projected at different levels of future scenarios. In general, as expected, the impacts were higher for the most extreme value of SLR150 (red lines in Figure 4), for which it is possible to assume a tide amplitude increasing in the upstream direction of the North and South channels. For the CS tide-monitoring gauge, the tidal range in north channel increased by about 16% compared to that in the current scenario for SLR150 (Figure 4, top). So, the progressive effect of the SLR tends to provoke a gradual increase in the tidal range as it propagates upstream. These findings confirm the hypothesis of [9] that the progressive effect of the SLR tends to provoke a gradual increase in the tidal range as it propagates upstream. In the present study, another observation was the relative delay of at least one hour in the flood and ebb times in the SLR150 scenario. This means that, in this scenario, the low and high waters tend to arrive earlier in the estuary.

3.2. Water Transport Time Scenarios along the Channel

Figure 6, showing the time behavior of surface water renewal rates (RTs), reports an RT of about 12 days during the wet regime and of around 29 days during the dry regime. The effect of an extreme sea level rise (SLR150) in the estuary was to prolong the RT to values of approximately 1 and 2 days during the wet and dry periods, respectively. These findings corroborate the results obtained with the Eulerian model available in the SISBAHIA, in which the transport time in relation to water age into the Amazon River estuary was simulated considering the impact of the SLR150 scenario. Comparing the spatial configuration of water age for the current (black solid lines) and future scenarios (red dotted lines) in Figure 7, we can observe that the red contours are positioned relatively in front of the black contours, indicating a tendency of temporal extension in the dynamics of the waters of around 1 day in the wet regime (Figure 7, left) and of about 2 days in the dry regime (Figure 7, right).

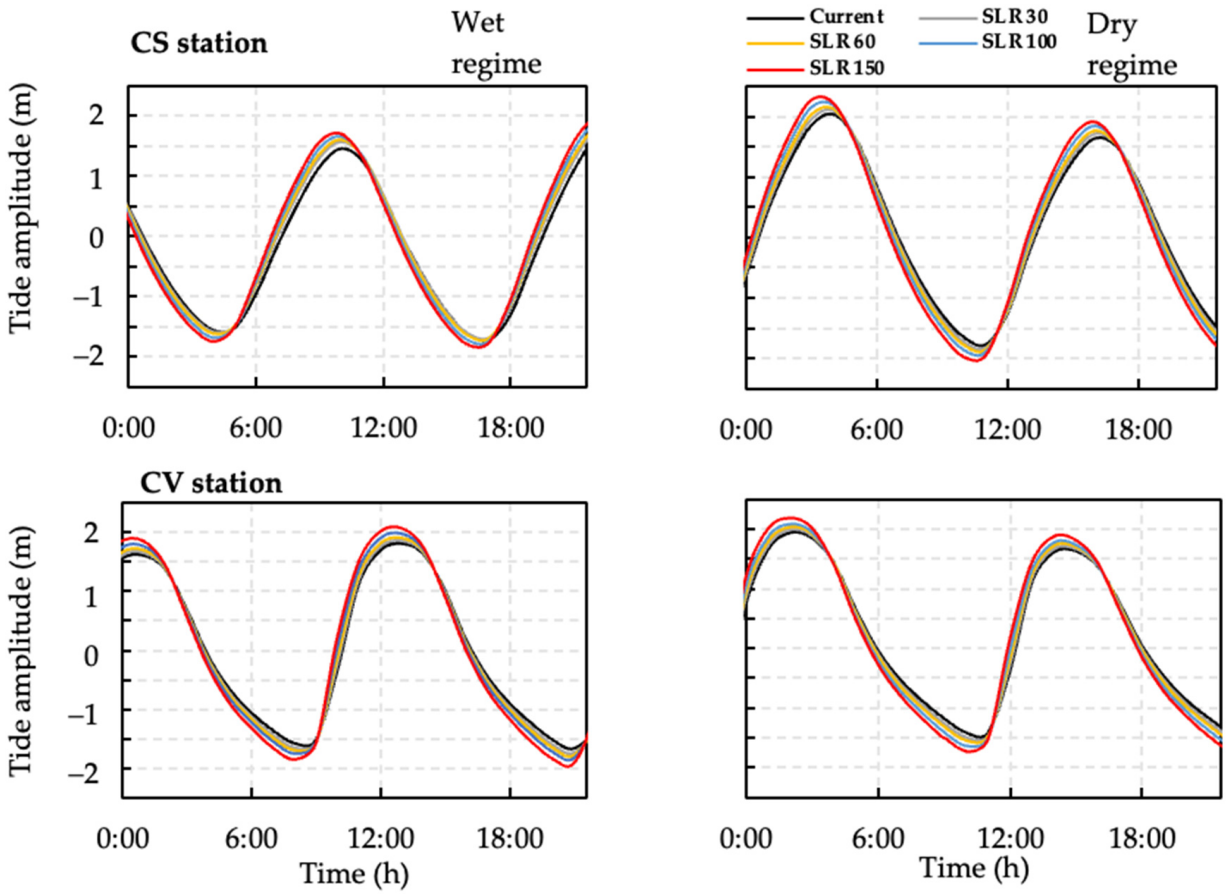

Figure 5. Diurnal variation of the tidal amplitude in the Amazon River estuary in the wet and dry regimes considering different SLR projections (colored lines) compared with the current data (black line) at the tide-monitoring gauges CS in the north channel (top) and CV in the south channel (bottom).

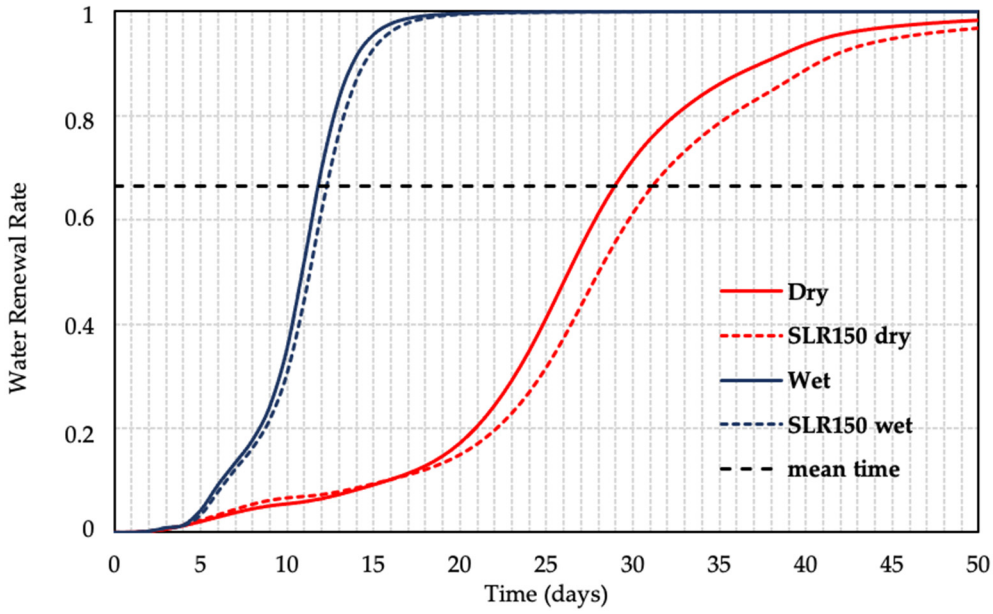

Figure 6. Variations in water renewal rate (RT) in the Amazon River estuary for the wet (in blue) and dry (in red) periods. Arrows indicate the direction of change in both seasonal periods.

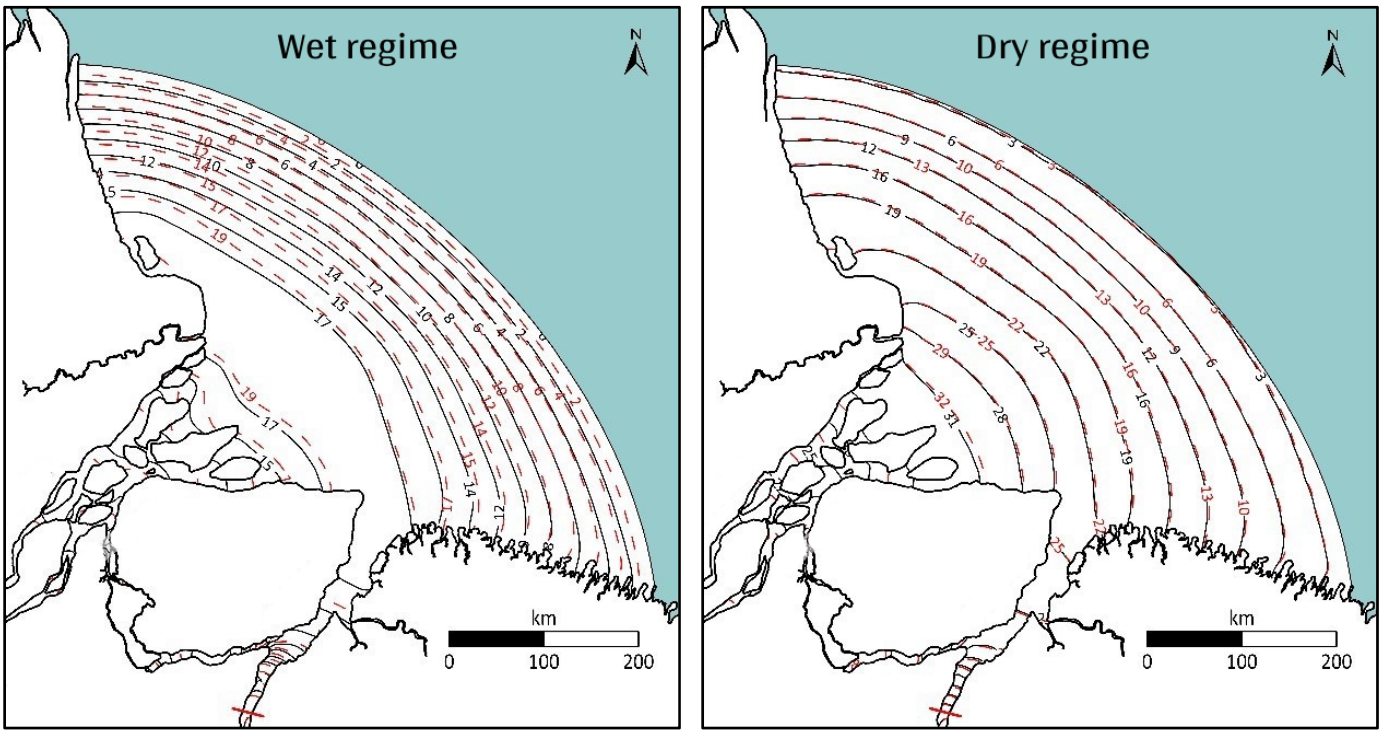

Figure 7. Water age (days) spatial patterns in the Amazon River estuary for the high flow during the wet regime (**left**) and for the low flow during the dry (**right**) regime. Black lines represent the current scenario, and red dashed lines represent the SLR150 scenario.

4. Discussion

Although the ocean force directs the coastal ecosystem, there are still many gaps in knowledge about how the sea influences estuary hydrodynamics. The west coast of the United States was studied, revealing that the rising sea levels will have numerous adverse effects on coastal biodiversity [40]. In this region of the north Atlantic, the SLR will have a disproportionate impact on the lower order of tidal streams and their terrestrial interfaces, so that 1 m in SLR variation will decrease the land–water tidal flow interface by 17% and the total surface area of U.S. tidal currents by 31%. Influences upstream of the tidal zones will be extended in response to the SLR, but the increase will be more than offset by coastal losses, because topographic gradients become steeper inland, and accretion rates may not keep up with the SLR. As discussed in [41], tidal amplification occurs due to the gradual decrease in the width and/or depth of the estuary. Hence, if much of the geomorphology of the Amazon River estuary remains unchanged, particularly in terms of hydrosediments [40,42,43], the rise in the mean sea level will expand the available crossflow area of entry. This expansion will impact the dynamics of estuarine tides, leading to a larger tidal prism [8]. This bigger tidal prism will alter the effect of friction, tidal wave propagation patterns and tidal current velocity [43]. Additionally, the sea level rise alters the asymmetry of tidal waves, a crucial factor for sediment transport, current effects, and secondary currents in meandering rivers. Tidal wave asymmetry generally refers to the phenomenon of tidal wave deformation, where the duration of ebb and flood tides is uneven [41]. In the Lower Amazon River, close to Macapá city, this asymmetry is already well known, varying both spatially and seasonally [11,14,16–18,44]. For instance, during the dry period in the North Channel, on average, the ebb lasts about 4.5 h, and the flood about 3.5 h, while during the rainy season, on average the ebb lasts about 8 h, and the flood about 4 h, according to the lunar phases and periods, generating in both seasons an asymmetry of tidal propagation [10,11].

Our simulation results indicating changes in the spatial dynamics of surface water renewal rates and water age over the Amazon estuary are consistent with scientific knowl-

edge of regional hydrodynamics. The Amazon River estuary has large bodies of water and a complex quantity of dissolved substances [11,18], which explains the relatively fast surface water renewal rates compared to those of other small estuaries, for both the wet and the dry seasons [17]. This is due to the change in the flow pattern in these periods by the modulation of the precipitation pattern in the watershed, caused in particular by the extreme climate events observed during the last decades [10,11,45,46].

The Amazon River estuary is surrounded by low plains that are below the high tide limit and form floodplain areas [47]. With the SLR effect, many areas with topography above the tidal ceiling will periodically become flooded, and the areas that are periodically flooded will be permanently flooded. The loss of these areas can result in reduced carbon uptake from the land and the release of carbon stored in peat that is decomposed in the aquatic environment [42,47]. More generally, given the significant contributions of these areas to the ecosystem's net productivity [11,14,18,22], the losses of these systems due to SLR could significantly impact the carbon cycle and other biogeochemical processes in coastal regions. In the end, we will have a positive-feedback situation, as changes in hydrodynamics can influence the emission of greenhouse gases (amplifying global warming), thus raising the mean sea level, which in turn will tend to further influence the hydrodynamic pattern of estuaries [14].

Increasing in water depths change the inundation patterns over a tidal cycle, increasing the tidal amplitude in the land direction, thus expanding the area suitable for establishing floodplain ecosystems. If the sediment supply decreases over time, the increase in water depth can increase the sediment capture rate in the system [11] and thus alter the geomorphology and dynamics of the system [47–49]. If the SLR rate exceeds the accretion capacity of the estuary (such as rainfall magnitude, location, response to capture and transport of cohesive sediment), a change in vegetation composition and open water cover is predictable, leading to further changes in estuarine dynamics [50,51]. In addition, losses or the intensification of hydraulic connectivity between flooded plains or between lakes and canals or large rivers would significantly change the evaporation rates of these water bodies and enhance salinization processes and significant changes in water quality [45,52–55]. As the tidal prism and water depth will likely increase under SLR, the extent of saline intrusion may increase, leading to the loss of freshwater ecosystems [52]. Indeed, any change in the salinity of estuarine water (as a component of water quality) can negatively impact estuarine flora and fauna communities [53] and the entire physical environment of the area in contact with the sea [38,54–58]. A recent issue currently occurring in the coastal zone of Amapá in the Amazon estuary concerns the intensification of the progressive erosion of a new tidal channel (Urucurituba) between the Amazon River and the Araguari River, which has recently generated significant geomorphological changes with strong impacts on the landscape and hydrodynamic patterns near the mouth of the Araguari River, altering the river's drainage system and the general water quality [49,54,55,59–62].

Concerning the potential impacts on the local tropical biodiversity of the SLR, the Amazonian estuary is considered environmentally sensitive when it comes to the coast [16]. About the aquatic biota, in addition to sheltering protected areas and several riverside communities, preventive protection against probable episodes involving potential accidents with ships and oil spills is especially relevant for the conservation of the Amazonian biodiversity [27,63]. In a recent study conducted in [27], the biological resources and endemic species present in the Lower Amazon River were mapped, covering approximately 60 sites. These findings will serve as a reference for assessing the current and future impacts of sea level rise on local biodiversity.

Aiming to contribute to the scientific discussion on the research theme, we elaborated a summarized schematic diagram (Figure 8) of the complex direct and indirect impacts of sea level rise on the hydrodynamic patterns in the Amazon estuary. Due to its unique shape and system boundary conditions and in response to the SLR impacts (first order), the estuary will exhibit alterations in tidal regime and renewal time of fluvial–maritime waters (second order). Subsequently, cascade processes can have impacts on some variables in the

dimensions of the environment and biogeochemistry (third order) that tend to manifest themselves on a longer (and more unpredictable) time scale, due to the slower nature of ecological and geomorphic responses [8,15,40,46,50,62]. In a long-term integrated perspective, systemic consequences are expected in terms of ecology and the environment, which can lead to an ecosystem imbalance. Thus, the final scenario of natural and anthropogenic pressures can aggravate the socio-environmental vulnerability in the face of natural disasters, directly affecting the activities of the productive sector and the regional socioeconomics. In Figure 8, the potential effects of changes in SLR according to different levels or orders of impact are summarized.

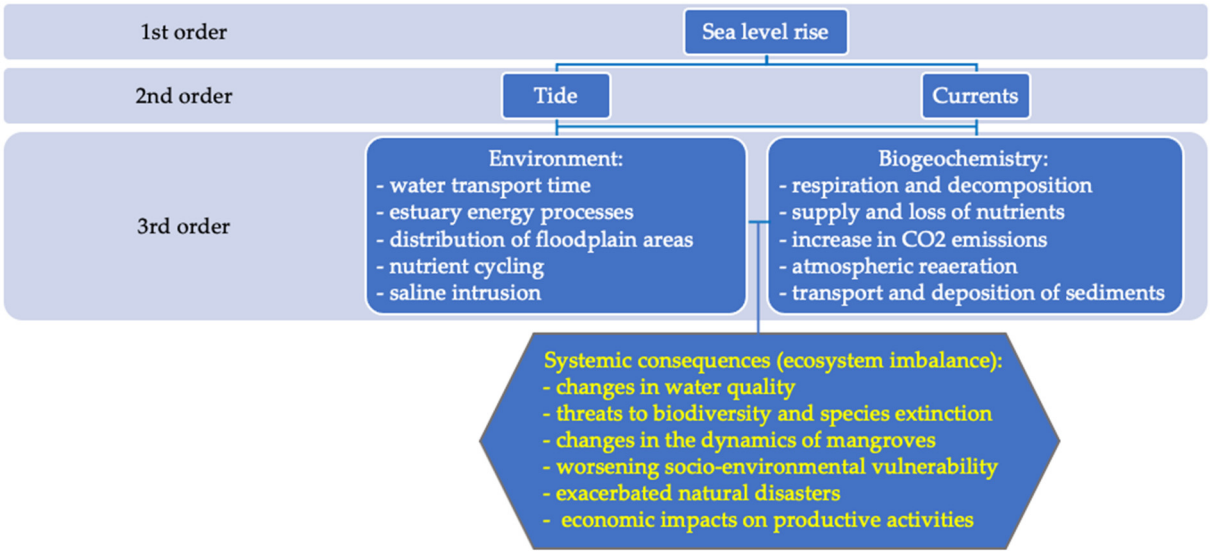

Figure 8. Schematic diagram of the first-, second- and third-order impacts of sea level rise on the hydrodynamic patterns in the low Amazon estuary, including systemic consequences for the environment and society.

Based on similar studies in the literature, we utilized a maximum projected sea level rise ranging from SLR = 150 cm to SLR = 2.0 m [8,56–62]. Furthermore, as mentioned earlier and for didactic purposes, our simulations indicated that SLR values ≥150 cm or up to 2.0 m were consistent with the maximum amplitudes reported in the literature. Therefore, it remains plausible to propose scenarios with "very extreme" variations, such as SLR = 2.0 m, particularly in the event of early instability of the Antarctic ice sheet [56]. Thus, the extreme sea level rise case of 1.5 m, as suggested by several publications [8,56,61,62], was also assessed.

Referring to Figure 8 schematic diagram, which illustrates the primary, secondary, and tertiary impacts of sea level rise on the hydrodynamic patterns within the Lower Amazon estuary, along with its systemic consequences for the environment and society, the following observations emerged [55–62]:

1. First-order effect: throughout the 21st century, sea level rise is expected to significantly impact the hydrodynamic balance in the Amazon River estuary, especially currents, tidal range, recirculation, sediment transport, water quality. But the response of a coastal region to sea level rise depends on the local physical characteristics, which must therefore be assessed to provide an accurate investigation of vulnerability [16,17,49,55].
2. Second-order effect: throughout the 21st century, sea level rise is expected to significantly impact the hydrodynamic balance in the Amazon River estuary [16,17,49], especially currents, tidal range, recirculation, sediment transport, water quality, and discernible alterations in water renewal rates throughout the estuary, persisting for approximately 2 days during the dry season ($p < 0.05$).

3. Third-order effect: (a) environmental, i.e., abnormal variations in water transport time (age and renewal rate) and energetic processes, mainly concerning erosion processes of coarse sediments, alteration in water surface distribution, including flooded plains, changes in nutrient cycling and saline intrusion; (b) biogeochemical, i.e., impacts on respiration and decomposition processes (CO_2 and CH_4 outgassing), fluctuations in nutrient supply and loss, rise in CO_2 and CH_4 outgassing, transport and deposition of sediments; (c) simultaneous processes, i.e., disruption of aquatic and terrestrial ecosystems, particularly in coastal and flooded plain areas, shifts in water quality affecting the aquatic fauna and fisheries, risks to aquatic biodiversity and species extinction, alterations in mangrove dynamics, increased socio-environmental vulnerability among traditional, riverside, and urban populations, intensification of extreme hydrological processes, economic ramifications of productive sectors and widespread environmental impacts. For example, climate change alone will drastically reshape the Lower Amazon River's functioning in the future, leading to increased coastal flooding and estuarine wetland submergence, heightened salinity variability on various time scales, more occurrences of harmful algae, elevated hypoxia levels, diminished dominant submerged aquatic vegetation, and altered interactions between trophic levels, favoring subtropical fish and shellfish species [10–24].

Climate change poses a significant threat to the global economy, particularly due to its severe impact on coastal ecosystems. Key factors include rising temperatures, alterations in precipitation patterns (duration, frequency, timing and intensity), heightened storm frequency and intensity, shifts in ocean currents and rising sea levels leading to salinization processes. These environmental pressures, compounded by increasing anthropogenic activities like pollution, land conversion and resource extraction, jeopardize the ecosystems, leading to shrinkage and degradation [55–63].

Brazil ranks among the top 15 nations most vulnerable to climate change impacts. It is imperative to safeguard, for example, the mangroves, which serve as a vital buffer against climate-related hazards. The mangrove forests play a pivotal role, offering essential benefits in adapting to climate impacts. Ensuring the preservation of the mangrove and estuarine ecosystems is essential for mitigating climate change-related risks [60,61].

Finally, it is crucial to acknowledge the limitations of the present study. Key constraints include (a) a limited number of long-term hydrological or tide gauge stations, some of which may have experienced significant interruptions; (b) the high costs associated with field campaigns, posing challenges in refining field monitoring and impacting the quality of the hydrological parameters used in numerical models (such as model calibration or validation); (c) the absence of readily available tools for modeling the hydrodynamic (shallow water) and climatic effects at the Amazon River mouth, hindering the integration of these two aspects (downscaling) [15,17,23,26,27].

5. Conclusions

Our fundamental hypothesis about significant changes in the hydrodynamic pattern, particularly space–time variations in the tide amplitude and the surface water renewal rates, along the Lower Amazon River estuary, because of the principal impact of long-term SLR induced by global climate change, was confirmed. The moderate geometric convergence of the channel was shown to provide a gradual increase in the tidal amplitude as it propagates upstream, whose effect can be corroborated by similar studies in the literature. Indeed, the current velocity pattern (time of ebb and flood tides), especially during the dry season) was significantly altered, and significant seasonal changes in the estuarine mass transport rates could occur, with impacts on the hydrodynamic pattern, exchange processes and land–water connectivity. As expected, the mean water renewal time in the estuary during the dry season (29 days) was longer than during the wet season (12 days). Therefore, with an extreme sea level rise of up to 150 cm projected by the end of the 21st century, the wet and dry season water renewal times would increase, respectively, by 1 and 2 days. In other words, the river entry would remain in the estuary longer after a rise in the sea level, which

could affect biogeochemical processes, mainly increasing the retention time of dissolved substances in the estuary.

Although the present research is an important contribution to the understanding of the impacts of SLR on the Amazon estuary, there are still limitations concerning historical tide series data and a need to carry out new campaigns for a more detailed refinement of the tidal variations, so that we can further advance our scientific understanding of the Amazon coastal hydrodynamics.

Author Contributions: Conceptualization, methodology, numerical modeling, formal analysis and writing—original draft preparation: J.L.P.C., C.H.M.d.A. and A.C.d.C.; writing—review and editing: E.B.d.S. and A.C.d.C.; supervision and project administration: E.B.d.S. and A.C.d.C. All authors have read and agreed to the published version of the manuscript.

Funding: This research was funded by the Federal University of Amapá (UNIFAP), the Amapá State University (UEAP), the National Council for Scientific and Technological Development—CNPQ (grant 314830/2021-9 and 313148/2020-1) and the Foundation Coordination for the Improvement of Higher Education Personnel (CAPES).

Data Availability Statement: All databases (sources and references) are described in the Section 2.

Acknowledgments: J.L.P.C was supported by a scholarship from CNPq (grant 309684/2018-8). The authors thank the Laboratory of Chemistry, Sanitation and Environmental Systems Modeling (LQSMSA), the Laboratory of Transport Phenomena and Hydraulics and Environmental Sanitation (LFTHSAM), CAPES for the scholarship, CNPQ for the research productivity grants (314830/2021-9 and 313148/2020-1) and DPq/PROPESPg/UNIFAP for the support in the graduate programs.

Conflicts of Interest: The authors declare no conflicts of interest.

References

1. Dangendorf, S.; Hay, C.; Calafat, F.M.; Marcos, M.; Piecuch, C.G.; Berk, K.; Jensen, J. Persistent acceleration in global sea-level rise since the 1960s. *Nat. Clim. Chang.* **2019**, *9*, 705–710. [CrossRef]
2. Church, J.A.; Clark, P.U.; Cazenave, A.; Gregory, J.M.; Jevrejeva, S.; Levermann, A.; Merrifield, M.A.; Milne, G.A.; Nerem, R.S.; Nunn, P.D.; et al. Sea Level Change. In *Climate Change 2013: The Physical Science Basis. Contribution of Working Group I to the Fifth Assessment Report of the Intergovernmental Panel on Climate Change*, 1st ed.; Stocker, T.F., Qin, D., Plattner, G.-K., Tignor, M., Allen, S.K., Boschung, J., Nauels, A., Xia, Y., Bex, V., Midgley, P.M., Eds.; Cambridge University Press: Cambridge, UK; New York, NY, USA, 2013.
3. Wong, T.E.; Bakker, A.M.R.; Keller, K. Impacts of Antarctic fast dynamics on sea-level projections and coastal flood defense. *Clim. Chang.* **2017**, *144*, 347–364. [CrossRef]
4. Frederikse, T.; Landerer, F.W.; Caron, L.; Adhikari, S.; Parkes, D.; Humphrey, V.; Dangendorf, S.; Hogarth, P.; Zanna, L.; Cheng, L.; et al. The causes of sea-level rise since 1900. *Nature* **2020**, *584*, 393–397. [CrossRef] [PubMed]
5. Chen, W.; Chen, K.; Kuang, C.; Zhu, D.Z.; He, L.; Mao, X.; Liang, H.; Song, H. Influence of sea level rise on saline water intrusion in the Yangtze River Estuary, China. *Appl. Ocean Res.* **2016**, *54*, 12–25. [CrossRef]
6. Hong, B.; Shen, J. Responses of estuarine salinity and transport processes to potential future sea-level rise in the Chesapeake Bay. *Estuar. Coast. Shelf Sci.* **2012**, *104–105*, 33–45. [CrossRef]
7. Chua, V.P.; Xu, M. Impacts of sea-level rise on estuarine circulation: An idealized estuary and San Francisco Bay. *J. Mar. Syst.* **2014**, *139*, 58–67. [CrossRef]
8. Hong, B.; Liu, Z.; Shen, J.; Wu, H.; Gong, W.; Xu, H.; Wang, D. Potential physical impacts of sea-level rise on the Pearl River Estuary, China. *J. Mar. Syst.* **2019**, *201*, 103245. [CrossRef]
9. Du, J.; Shen, J.; Zhang, Y.J.; Ye, F.; Liu, Z.; Wang, Z.; Wang, Y.P.; Yu, X.; Sisson, M.; Wang, H.V. Tidal Response to Sea-Level Rise in Different Types of Estuaries: The Importance of Length, Bathymetry, and Geometry. *Geophys. Res. Lett.* **2018**, *45*, 227–235. [CrossRef]
10. Less, D.F.; Cunha, A.C.; Sawakuchi, H.O.; Neu, V.; Valério, A.M.; Ward, N.D.; Abreu, C.M. The role of hydrodynamic and bi-ogeochemistry on CO_2 flux and pCO_2 at the Amazon River mouth. *Biogeosci. Discuss.* **2018**, *465*, 1–26. [CrossRef]
11. Ward, N.D.; Sawakuchi, H.O.; Neu, V.; Less, D.F.S.; Valerio, A.M.; Cunha, A.C.; Kampel, M.; Bianchi, T.S.; Krusche, A.V.; Richey, J.E.; et al. Velocity-amplified microbial respiration rates in the lower Amazon River. *Limnol. Oceanogr. Lett.* **2018**, *3*, 265–274. [CrossRef]
12. Raymond, P.A.; Hartmann, J.; Lauerwald, R.; Sobek, S.; McDonald, C.; Hoover, M.; Butman, D.; Striegl, R.; Mayorga, E.; Humborg, C.; et al. Global carbon dioxide emissions from inland waters. *Nature* **2013**, *503*, 355–359. [CrossRef] [PubMed]
13. Richey, J.E.; Hedges, J.I.; Devol, A.H.; Quay, P.D.; Victoria, R.; Martinelli, L.; Forsberg, B.R. Biogeochemistry of carbon in the Amazon River. *Limnol. Oceanogr.* **1990**, *35*, 352–371. [CrossRef]

14. Sawakuchi, H.O.; Neu, V.; Ward, N.D.; Barros, M.d.L.C.; Valerio, A.M.; Gagne-Maynard, W.; Cunha, A.C.; Less, D.F.S.; Diniz, J.E.M.; Brito, D.C.; et al. Carbon Dioxide Emissions along the Lower Amazon River. *Front. Mar. Sci.* **2017**, *4*, 00076. [CrossRef]
15. Coles, V.J.; Brooks, M.T.; Hopkins, J.; Stukel, M.R.; Yager, P.L.; Hood, R.R. The pathways and properties of the Amazon River Plume in the tropical North Atlantic Ocean. *J. Geophys. Res. Oceans* **2013**, *118*, 6894–6913. [CrossRef]
16. Da Cunha, A.C.; De Abreu, C.H.M.; Crizanto, J.L.P.; Cunha, H.F.A.; Brito, A.U.; Pereira, N.N. Modeling pollutant dispersion scenarios in high vessel-traffic areas of the Lower Amazon River. *Mar. Pollut. Bull.* **2021**, *168*, 112404. [CrossRef]
17. de Abreu, C.H.M.; Barros, M.d.L.C.; Brito, D.C.; Teixeira, M.R.; da Cunha, A.C. Hydrodynamic Modeling and Simulation of Water Residence Time in the Estuary of the Lower Amazon River. *Water* **2020**, *12*, 660. [CrossRef]
18. Ward, N.D.; Keil, R.G.; Medeiros, P.M.; Brito, D.C.; Cunha, A.C.; Dittmar, T.; Yager, P.L.; Krusche, A.V.; Richey, J.E. Degradation of terrestrially derived macromolecules in the Amazon River. *Nat. Geosci.* **2013**, *6*, 530–533. [CrossRef]
19. Keil, R.G.; Mayer, L.M.; Quay, P.D.; Richey, J.E.; Hedges, J.I. Loss of organic matter from riverine particles in deltas. *Geochim. Cosmochim. Acta* **1997**, *61*, 1507–1511. [CrossRef]
20. Medeiros, P.M.; Seidel, M.; Dittmar, T.; Whitman, W.B.; Moran, M.A. Drought-induced variability in dissolved organic matter composition in a marsh-dominated estuary. *Geophys. Res. Lett.* **2015**, *42*, 6446–6453. [CrossRef]
21. Valerio, A.M.; Kampel, M.; Ward, N.D.; Sawakuchi, H.O.; Cunha, A.C.; Richey, J.E. CO_2 partial pressure and fluxes in the Amazon River plume using in situ and remote sensing data. *Cont. Shelf Res.* **2021**, *215*, 104348. [CrossRef]
22. Abril, G.; Martinez, J.-M.; Artigas, L.F.; Moreira-Turcq, P.; Benedetti, M.F.; Vidal, L.; Meziane, T.; Kim, J.-H.; Bernardes, M.C.; Savoye, N.; et al. Amazon River carbon dioxide outgassing fuelled by wetlands. *Nature* **2013**, *505*, 395–398. [CrossRef] [PubMed]
23. da Cunha, A.C.; Mustin, K.; dos Santos, E.S.; dos Santos, W.G.; Guedes, M.C.; Cunha, H.F.A.; Rosman, P.C.C.; Sternberg, L.d.S.L. Hydrodynamics and seed dispersal in the lower Amazon. *Freshw. Biol.* **2017**, *62*, 1721–1729. [CrossRef]
24. Khojasteh, D.; Glamore, W.; Heimhuber, V.; Felder, S. Sea level rise impacts on estuarine dynamics: A review. *Sci. Total Environ.* **2021**, *780*, 146470. [CrossRef] [PubMed]
25. Jahandideh-Tehrani, M.; Zhang, H.; Helfer, F.; Yu, Y. Review of climate change impacts on predicted river streamflow in tropical rivers. *Environ. Monit. Assess.* **2019**, *191*, 752. [CrossRef]
26. Rosman, P.C.C. Referencia Tewcnica do Sisbahia-Sistema Base de Hidrodinamica Ambiental, Programa COPPE. Engenharia Oceanica: Area de Engenharia Costeira e Oceanografica, Rio De Janeiro, Brasil. 2018. Available online: http://www.sisbahia.coppe.ufrj.br (accessed on 2 June 2021).
27. Araújo, E.P.; de Abreu, C.H.M.; Cunha, H.F.A.; Brito, A.U.; Pereira, N.N.; da Cunha, A.C. Vulnerability of biological resources to potential oil spills in the Lower Amazon River, Amapá, Brazil. *Environ. Sci. Pollut. Res.* **2022**, *30*, 35430–35449. [CrossRef] [PubMed]
28. Gallo, M.N.; Vinzon, S.B. Generation of overtides and compound tides in Amazon estuary. *Ocean Dyn.* **2005**, *55*, 441–448. [CrossRef]
29. Molinas, E.; Vinzon, S.B.; Vilela, C.d.P.X.; Gallo, M.N. Structure and position of the bottom salinity front in the Amazon Estuary. *Ocean Dyn.* **2014**, *64*, 1583–1599. [CrossRef]
30. de Souza, E.B.; Cunha, A.C. Climatologia de precipitação no Amapá e mecanismos climáticos de grande escala. In *Tempo, Clima e Recursos Hídricos: Resultados do Projeto Remetap no Estado do Amapá*, 1st ed.; Cunha, A.C., de Souza, E.B., Cunha, H.F.A., Eds.; IEPA: Macapá, AP, Brazil, 2010; pp. 177–195.
31. Kottek, M.; Grieser, J.; Beck, C.; Rudolf, B.; Rubel, F. World map of the Köppen-Geiger climate classification updated. *Meteorol. Z.* **2006**, *15*, 259–263. [CrossRef] [PubMed]
32. Costa, A.C.L.; Rodrigues, H.J.B.; Silva Junior, J.A.; Nunes, L.R.C.; Moraes, B.C.; Costa, A.C.; Malhi, Y.S. Hourly, Daily and Seasonal Frequency Variability and Precipitation Intensity in a Rainy Tropical Rainforest in the Brazilian Amazon. *Rev. Bras. Geogr. Física* **2018**, *11*, 1290–1302. [CrossRef]
33. De Souza, E.B.; Ferreira, D.B.d.S.; Guimarães, J.T.F.; Franco, V.D.S.; de Azevedo, F.T.M.; de Moraes, B.C.; Souza, P.J.P. Padrões climatológicos e tendências da precipitação nos regimes chuvoso e seco da Amazônia oriental. *Rev. Bras. Climatol.* **2017**, *21*, 81–93. [CrossRef]
34. Moss, R.H.; Edmonds, J.A.; Hibbard, K.A.; Manning, M.R.; Rose, S.K.; Van Vuuren, D.P.; Carter, T.R.; Emori, S.; Kainuma, M.; Kram, T. The next generation of scenarios for climate change research and assessment. *Nature* **2010**, *463*, 747–756. Available online: https://www.nature.com/articles/nature08823 (accessed on 7 December 2018). [CrossRef] [PubMed]
35. Van Vuuren, D.P.; Edmonds, J.; Kainuma, M.; Riahi, K.; Thomson, A.; Hibbard, K.; Hurtt, G.C.; Kram, T.; Krey, V.; Lamarque, J.-F.; et al. The representative concentration pathways: An overview. *Clim. Chang.* **2011**, *109*, 5–31. [CrossRef]
36. Kjerfve, B. Estuarine geomorphology and physical oceanography. In *Estuarine Ecology*; Day, J.W., Hall, C.A.S., Kemp, W.M., Yáñez-Arancibia, A., Eds.; Wiley: New York, NY, USA, 1989; pp. 47–78.
37. Gabioux, M.; Vinzon, S.B.; Paiva, A.M. Tidal propagation over fluid mud layers on the Amazon shelf. *Cont. Shelf Res.* **2005**, *25*, 113–125. [CrossRef]
38. Prestes, Y.O.; Borba, T.A.; da Silva, A.C.; Rollnic, M. A discharge stationary model for the Pará-Amazon estuarine system. *J. Hydrol. Reg. Stud.* **2020**, *28*, 100668. [CrossRef]
39. Fassoni-Andrade, A.C.; Durand, F.; Moreira, D.; Azevedo, A.; dos Santos, V.F.; Funi, C.; Laraque, A. Comprehensive bathymetry and intertidal topography of the Amazon estuary. *Earth Syst. Sci. Data* **2021**, *13*, 2275–2291. [CrossRef]

40. Tagestad, J.; Ward, N.D.; Butman, D.; Stegen, J. Small streams dominate US tidal reaches and will be disproportionately impacted by sea-level rise. *Sci. Total Environ.* **2020**, *753*, 141944. [CrossRef] [PubMed]
41. van Rijn, L.C. Analytical and numerical analysis of tides and salinities in estuaries; part I: Tidal wave propagation in convergent estuaries. *Ocean Dyn.* **2011**, *61*, 1719–1741. [CrossRef]
42. Nittrouer, C.A.; DeMaster, D.J.; Kuehl, S.A.; Figueiredo, A.G., Jr.; Sternberg, R.W.; Faria, L.E.C.; Silveira, O.M.; Allison, M.A.; Kineke, G.C.; Ogston, A.S.; et al. Amazon Sediment Transport and Accumulation Along the Continuum of Mixed Fluvial and Marine Processes. *Annu. Rev. Mar. Sci.* **2021**, *13*, 501–536. [CrossRef]
43. Khojasteh, D.; Hottinger, S.; Felder, S.; De Cesare, G.; Heimhuber, V.; Hanslow, D.J.; Glamore, W. Estuarine tidal response to sea level rise: The significance of entrance restriction. *Estuar. Coast. Shelf Sci.* **2020**, *244*, 106941. [CrossRef]
44. Ward, N.D.; Morrison, E.S.; Liu, Y.; Rivas-Ubach, A.; Osborne, T.Z.; Ogram, A.V.; Bianchi, T.S. Marine microbial community responses related to wetland carbon mobilization in the coastal zone. *Limnol. Oceanogr. Lett.* **2018**, *4*, 25–33. [CrossRef]
45. da Cunha, A.C.; Sternberg, L.d.S.L. Using stable isotopes ^{18}O and ^{2}H of lake water and biogeochemical analysis to identify factors affecting water quality in four estuarine Amazonian shallow lakes. *Hydrol. Process.* **2018**, *32*, 1188–1201. [CrossRef]
46. Lewis, S.L.; Brando, P.M.; Phillips, O.L.; van der Heijden, G.M.F.; Nepstad, D. The 2010 Amazon Drought. *Science* **2011**, *331*, 554. [CrossRef] [PubMed]
47. Zeng, N.; Yoon, J.-H.; Marengo, J.; Subramaniam, A.; Nobre, C.; Mariotti, A.; Neelin, J.D. Causes and impacts of the 2005 Amazon drought. *Environ. Res. Lett.* **2008**, *3*, 014002. [CrossRef]
48. Fricke, A.T.; Nittrouer, C.A.; Ogston, A.S.; Nowacki, D.J.; Asp, N.E.; Filho, P.W.M.S. Morphology and dynamics of the intertidal floodplain along the Amazon tidal river. *Earth Surf. Process. Landf.* **2018**, *44*, 204–218. [CrossRef]
49. dos Santos, E.S.; Lopes, P.P.P.; Pereira, H.H.; Nascimento, O.O.; Rennie, C.D.; Sternberg, L.O.; da Cunha, A.C. The impact of channel capture on estuarine hydro-morphodynamics and water quality in the Amazon delta. *Sci. Total Environ.* **2018**, *624*, 887–899. [CrossRef] [PubMed]
50. Rayner, D.; Glamore, W.; Grandquist, L.; Ruprecht, J.; Waddington, K.; Khojasteh, D. Intertidal wetland vegetation dynamics under rising sea levels. *Sci. Total Environ.* **2020**, *766*, 144237. [CrossRef] [PubMed]
51. Sadat-Noori, M.; Rankin, C.; Rayner, D.; Heimhuber, V.; Gaston, T.; Drummond, C.; Chalmers, A.; Khojasteh, D.; Glamore, W. Coastal wetlands can be saved from sea level rise by recreating past tidal regimes. *Sci. Rep.* **2021**, *11*, 1196. [CrossRef] [PubMed]
52. Ensign, S.H.; Noe, G.B. Tidal extension and sea-level rise: Recommendations for a research agenda. *Front. Ecol. Environ.* **2018**, *16*, 37–43. [CrossRef]
53. Xiao, H.; Wang, D.; Medeiros, S.C.; Hagen, S.C.; Hall, C.R. Assessing sea-level rise impact on saltwater intrusion into the root zone of a geo-typical area in coastal east-central Florida. *Sci. Total Environ.* **2018**, *630*, 211–221. [CrossRef]
54. da Silva, G.C.X.; de Abreu, C.H.M.; Ward, N.D.; Belucio, L.P.; Brito, D.C.; Cunha, H.F.A.; da Cunha, A.C. Environmental Impacts of Dam Reservoir Filling in the East Amazon. *Front. Water* **2020**, *2*, 00011. [CrossRef]
55. Sousa, T.S.; Araújo, E.P.; da Cunha, A.C. Water surface variability in oceanic and estuarine coasts of Amapá, Brazil. *Aquat. Sci.* **2024**, *86*, 45. [CrossRef]
56. Kulp, S.A.; Strauss, B.H. New elevation data triple estimates of global vulnerability to sea-level rise and coastal flooding. *Nat. Commun.* **2019**, *10*, 4844. [CrossRef] [PubMed]
57. Leuliette, E.; Willis, J. Balancing the Sea Level Budget. *Oceanography* **2011**, *24*, 122–129. [CrossRef]
58. Watson, C.S.; White, N.J.; Church, J.A.; King, M.A.; Burgette, R.J.; Legresy, B. Unabated global mean sea-level rise over the satellite altimeter era. *Nat. Clim. Chang.* **2015**, *5*, 565–568. [CrossRef]
59. Cohen, M.C.L.; Alves, I.C.C.; França, M.C.; Pessenda, L.C.R.; Rossetti, D.d.F. Relative sea-level and climatic changes in the Amazon littoral during the last 500 years. *Catena* **2015**, *133*, 441–451. [CrossRef]
60. Suguio, K.; Martin, L.; Flexor, J.M. Quaternary Sea Levels of the Brazilian Coast: Recen Progress. *J. Int. Geosci.* **1988**, *11*, 203–208. [CrossRef]
61. Ward, R.D.; de Lacerda, L.D.; Cerqueira, A.d.S.; Silva, V.H.M.C.; Hernandez, O.C. Vertical accretion rates of mangroves in northeast Brazil: Implications for future responses and management. *Estuar. Coast. Shelf Sci.* **2023**, *289*, 108382. [CrossRef]
62. Najjar, R.G.; Pyke, C.R.; Adams, M.B.; Breitburg, D.; Hershner, C.; Kemp, M.; Howarth, R.; Mulholland, M.R.; Paolisso, M.; Secor, D.; et al. Potential climate-change impacts on the Chesapeake Bay. *Estuar. Coast. Shelf Sci.* **2010**, *86*, 1–20. [CrossRef]
63. Demoner, S.C.; Abreu, C.H.M.; Teixeira, M.R.; Cunha, A.C. Numerical simulation of oil spills in the lower Amazon River. *Water* **2023**, *15*, 2197. [CrossRef]